

Supporting Information

for

Comment on “Determination of Nucleus Density in Semicrystalline Polymers from Nonisothermal Crystallization Curves”

José A. Martins

Departamento de Engenharia de Polímeros

Campus de Azurém

4800 058 Guimarães

Portugal

jamartins@dep.uminho.pt

Contents:

Supporting Text

Figures S1, S1, S3, S4

Supporting References

Supporting Text

This text presents a summary of the procedure described with detail in previous works to evaluate the nucleation density in polymers crystallizing in the absence of flow. This evaluation was done by relating local and global crystallization experimental results. The former, performed in a hot-stage coupled to an optical microscope, provides information on the spherulite growth rate. The latter allows recording the overall crystallization kinetics.

Regardless the nucleation type, instantaneous or sporadic, as demonstrated in Fig. S1, there is always significant impingement between spherulites, long before the attainment of the half-crystallization time. In the framework of Avrami's equation for an instantaneous nucleation of spheres, accounting for the effect of impingement between spherulites in the solidification process implies the following relation between $t_{50\%}$ and k

$$t_{50\%}^{-1} = \left(\frac{k}{\ln 2} \right)^{1/3} = \left(\frac{4\pi\rho_s}{3\rho_l} \frac{\bar{N}}{\ln 2} \right)^{1/3} G. \quad (S1)$$

At high temperatures, nucleation (either primary or secondary) is the slowest process, and this temperature dependence is generally expressed by

$$t_{50\%}^{-1} \propto G \propto \exp\left(-\frac{K_g}{T\Delta T f}\right). \quad (S2)$$

To explain the different slopes - K_g - values, as well as the vertical shift, when $\ln(t_{50\%}^{-1})$ and $\ln(G)$ are both plotted as function of $(T \Delta T f)^{-1}$, as shown in Fig. S2a, a dependence of the nucleation density on the temperature has to be considered. It was neglected in a latter work⁸ that obtained a similar relationship for estimating the nucleation density by coupling global and local crystallization experimental results. Problems with the reasoning there used were mentioned in the main paper. Establishment of this dependency is crucial for assigning a physical meaning to the obtained final result.

Crystallization models, such as Avrami's equation, do not explicitly consider this dependence. It is aggregated, together with the temperature dependence of G , in the k parameter.

It was assumed that the temperature dependence of \bar{N} is proportional to the probability of formation of a nuclei with critical size, that this nuclei develops in a heterogeneous substrate, and that this development is coherent with the substrate.² The proportionality factor, although

important from both an experimental and theoretical point of view, because it determines the maximum attainable nucleation density, is not relevant here since, as shown below, it is included in the pre-exponential factor of $(t_{50\%}^{-1})_0$. A more detailed accounting for this dependence was given in ref. S1, where an equilibrium distribution of nuclei is evaluated.

Assuming then that

$$\bar{N} \propto \exp\left(-\frac{K_n}{T\Delta T f}\right), \quad (\text{S3})$$

eq. (S1) may be written as

$$\ln t_{50\%}^{-1} = \ln(t_{50\%}^{-1})_0 - \frac{\Delta G_d}{RT} - \left(\frac{K_n}{3T\Delta T f} + \frac{K_g}{T\Delta T f}\right), \quad (\text{S4})$$

or, since $K_n = K_g \equiv K_g^G$ (because of the same nucleation type and coherence with the substrate),

$$\ln t_{50\%}^{-1} = \ln(t_{50\%}^{-1})_0 - \frac{\Delta G_d}{RT} - \left(\frac{K_g^{1/t_{50\%}}}{T\Delta T f}\right), \quad (\text{S5})$$

with

$$\ln(t_{50\%}^{-1})_0 = \frac{1}{3} \ln\left(\frac{4\pi\rho_s}{3\rho_l} \frac{N_0}{\ln 2}\right) + \ln G_0,$$

and

$$K_g^{1/t_{50\%}} = \frac{4}{3} K_g^G, \quad (\text{S6})$$

where K_g^G is the slope of $\ln(G)$ as function of $(T\Delta T f)^{-1}$.

Equation (S6) can be used as a gauge to infer the nucleation type and the dimensionality of the growing structure from experimental DSC and optical microscopy data. This inferring is free from model assumptions, other than that both nucleation and growth are interface controlled processes involving the same interface energies. For an instantaneous nucleation of structures having the spherical shape, the ratio between the two, expressed by eq. (S6) is 1.333. For POM and iPP in Fig. S2a, that ratio is 1.12 and 1.253, respectively^{2,3}, while for other polymers, such as MPDE, it is 1.283.²

The vertical shift between $\ln(t_{50\%}^{-1})$ and $\ln(G)$ yields the semi-empirical nucleation density variation with

$$\bar{N}_t = \frac{3\ln(2)}{4\pi} \left\{ \left(\frac{(t_{50\%}^{-1})_0}{G_0} \right)^3 + \exp \left[\frac{3(K_g^G - K_g^{1/t_{50\%}})}{T\Delta T f} \right] \right\}, \quad (S7)$$

which is eq. (13) of ref. 2. Figure S2b shows predictions confirmed by experimental data. Differences between them are more perceptible at lower crystallization temperatures and may be assigned to the DSC instrument's lack of sensitivity for detecting the heat released at the very earlier crystallization stages.

Extension of this procedure to nonisothermal experiments was also performed.³ The nonisothermal crystallization data was corrected for the calibration on cooling and for the heat released during the crystallization (both isothermal and nonisothermal). None of these two corrections was considered by the authors in refs. 1 and 8. A temperature $T_{50\%}$, corresponding to the half of the phase change, was evaluated, and its value was located in the plots in Fig. 2a, from which a nucleation density was estimated – Fig. S3. The values obtained were then compared with others evaluated from plastic parts processed by rotational moulding, enabling a prediction of the final spherulite size illustrated in Fig. S3. Application of this procedure to injection moulding parts, would be, at best, limited to the core spherulitic structure, even though requiring knowledge of the cooling rate at different sections of the part.

Although the nucleation density might change for different iPP grades, depending on the nucleating agents used, its dependency on the supercooling degree is illustrated in Fig. 5 of ref. 16. From data in that figure it can be seen that predicted nucleation density for a quiescent crystallization at 132 °C ($\log \Delta T \approx 1.9$) is higher than 10^{10} nuclei/m³ and that corresponding to 113 °C ($\log \Delta T \approx 2.0$) is around 10^{13} nuclei/m³, far above than the estimate made in Fig. 6 of ref. 1.

Since one reviewer raised doubts on the applicability of combined DSC and optical microscopy results to predict the nucleation density in nonisothermal experiments, arguing that the above procedure is “not on sound scientific foundation” because “under temperature gradients polymers exhibit directional crystallization” and “when confined by DSC pans, the surface nucleation plays a significant role in crystallization”, the following clarifications are in order.

The only way to ascertain the validity of a predictive method, and therefore its scientific foundations, is to compare their predictions with experimental results for a variety of materials as wide as possible, and for different working conditions, in this case, isothermal and nonisothermal

crystallization experiments in the absence of flow. Squares and circles in figs. S2b and S3 are nucleation density values measured on microtomed sections of samples crystallized in a DSC under isothermal or non-isothermal conditions. The measurements were made either by SALS or by the method described in Fig. S4. SALS measurements yield a mean spherulite diameter, representative of all structures hit by the spot (including eventual surface nuclei), from which a nucleation density can be directly evaluated. As can be seen, predictions compare well with experimental results. Those predictions were also extended to 10 mm thick plastic parts processed by rotational moulding.³ The cooling rates at 1 mm, 3 mm, 5 mm, 7 mm and 9 mm from the mould wall were measured by thermocouples inserted in the plastic part. From these cooling rates, a temperature $T_{50\%}$ corresponding to half of the phase change was evaluated, and using eq. (S.7) the nucleation density was predicted.

For samples of thickness around 1 mm, and in the absence of any thermal event in the sample, the temperature difference between the sample bottom and top, exclusively due to the sample's thermal resistance, is around 2 °C for highest cooling rate used (≈ -32 °C/min).⁴ The thermal gradients existing in DSC samples cooled at -32 °C/min are then around 2 °C/mm. The combined effects of the sample thermal resistance and heat of crystallization released during the phase change may be evaluated (see Fig. 10 in ref. S2) and, for each cooling rate a $T_{50\%}$ defined and used as above to estimate the nucleation density. So far, all known estimates made following the above procedure agreed with experimental nucleation density results (within the error bars, as shown in Fig S3).

As for the scientific foundations of the method, the following has to be said. Global crystallization experiments such as those performed in a DSC measure the heat released during the phase change at a predefined temperature or cooling rate. To describe the integrated results, different physically sound models may be used. One most used is the Avrami's equation. The kinetic constant of the Avrami's equation is proportional to $\bar{N}G^3$. It turns out that Avrami's model implicitly considers \bar{N} (the nucleation density) as a temperature independent value. It is known from experiments that increasing the supercooling degree increases the nucleation density.

The modification made that allowed the implementation of the predictive method and writing eq. (S7) was to assume that the temperature dependence of \bar{N} is proportional to the probability

of formation of a nuclei with critical size, that this nuclei develops in a heterogeneous substrate, and that this development is coherent with the substrate.

Despite the good agreement of eq. (S.7) with experimental results for the nucleation density, this procedure is not of universal validity. Extension of this methodology to samples crystallized at very low supercoolings will fail due to the extensive development of transcrystalline layers as a result of the enhanced surface nucleation. Still to explore, is the application of this procedure to predict the nucleation density in samples crystallizing at very high cooling rates, or to crystallizations from the glass. For flow induced crystallization processes, this method might eventually work for predicting the mean spherulite size of the core spherulitic structures in injection moulded parts providing that mean cooling rates could be defined at different sections of the part.

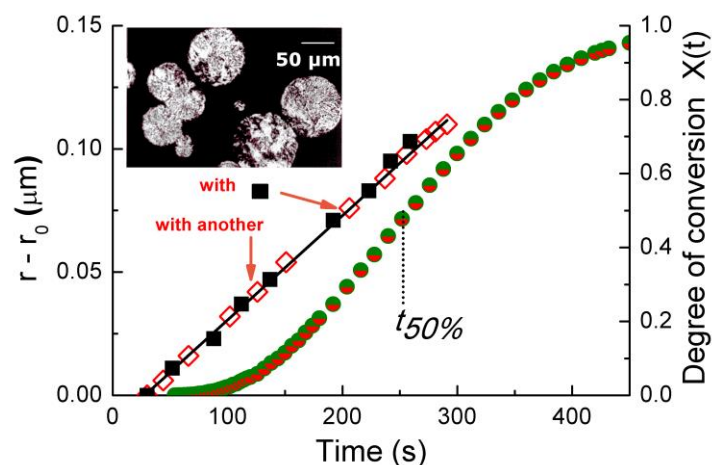


Figure S1. Isothermal crystallization of polyoxymethylene at 157 °C in a hot-stage and in a DSC. Time zero was set at the start of the isothermal in both instruments. The picture at the inset was taken in a polarized optical microscope during the crystallization at 157 °C and it corresponds to a crystallization time of 235 s. Diamonds and squares refer to measurements on the two spherulites at the lower right. The transformed area in the figure is around 45%. The impingement between spherulites is evident long before the half of crystallization time as it is evident the sporadic nature of the nucleation in POM at 157 °C.

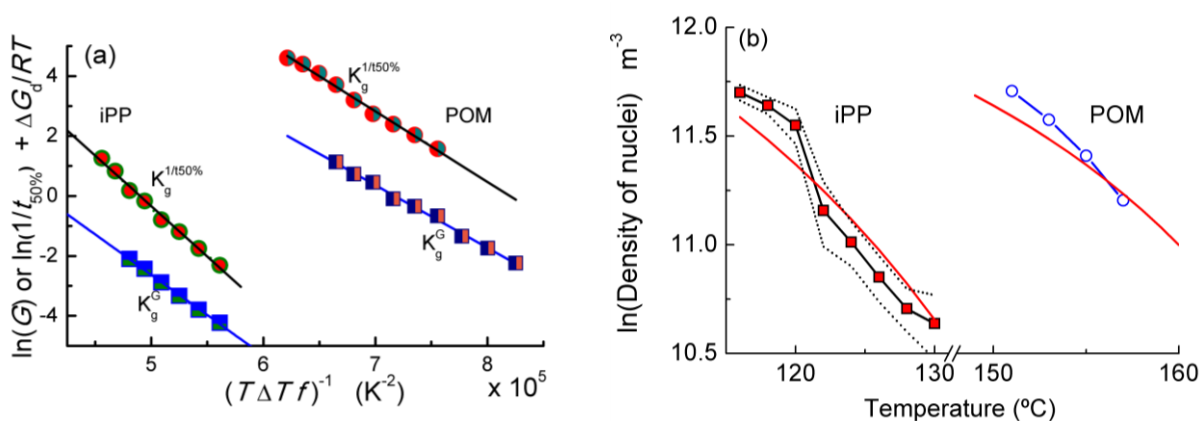


Figure S2. Use of combined DSC and optical microscopy data to evaluate the nucleation density. (a) Representation of the spherulite growth rate data and reciprocal of half crystallization time at different crystallization temperatures for POM² and iPP.³ The vertical shift between $\ln(1/t_{50\%}^{-1})$ and $\ln(G)$ yields the nucleation density represented in (b). Dotted lines in (b) indicate the errors in the experimental nucleation density evaluation of iPP (squares) and POM (circles), which was made by analysing microtomed sections of crystallized DSC samples.

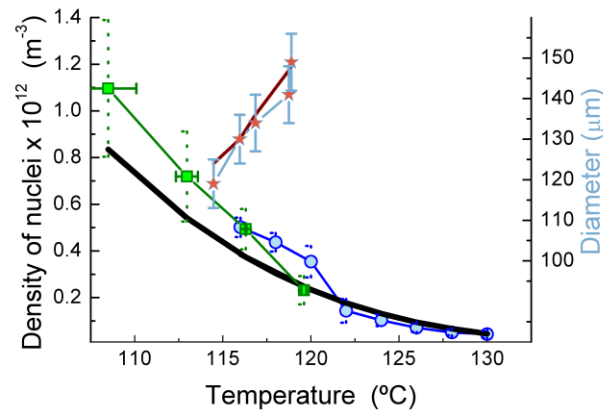


Figure S3. Prediction of nucleation density for isothermal and nonisothermal experiments and its use for evaluating the final mean spherulite diameter in real processing conditions. Black thick line is the prediction in a wide temperature range encompassing both isothermal and nonisothermal experiments. Squares are experimental evaluations for the nucleation density made for nonisothermal experiments at cooling rates from -5 °C/min up to -32 °C/min. Samples were crystallized in a DSC at the above cooling rates, and the microtomed sections analysed either by SALS or by the method described in Fig. S4. The corresponding temperatures were evaluated at half of the solidification process ($T_{50\%}$). The vertical error bars results represent errors in the evaluation of the nucleation density while the horizontal error bars stand for the combination of calibration on cooling errors and the sample thermal resistance effect on the $T_{50\%}$ definition. Circles are the experimental nucleation density values for isothermal experiments already presented in Fig. 2b. Measurements of the final spherulite size in parts processed by rotational moulding are shown by stars while the line is the corresponding prediction.³

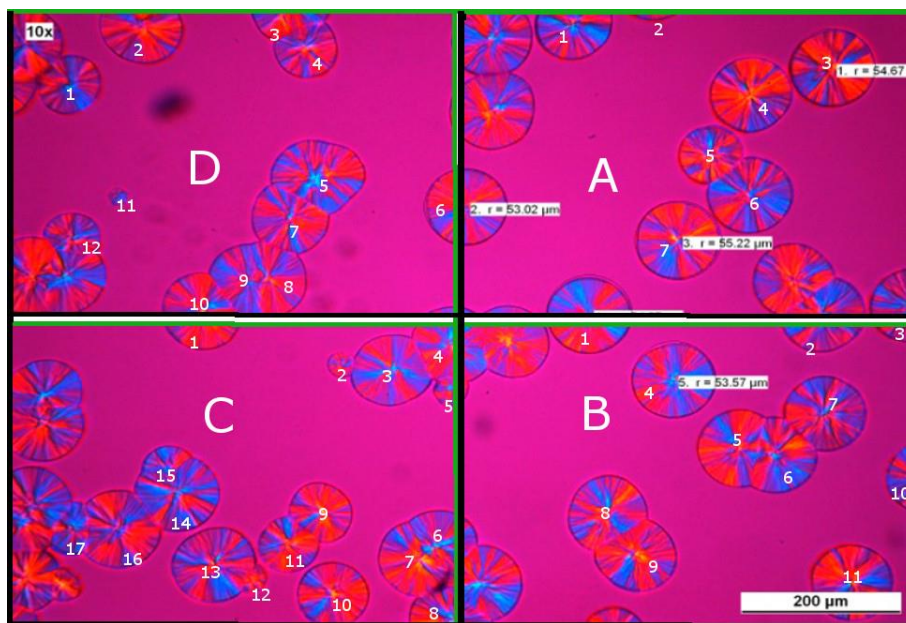


Figure S4. Figure 2 of ref. 1 for the isothermal crystallization at 132 °C. To evaluate the nucleation density, the figure was divided in four equal sections A to D. For each section acceptance lines (green) and forbidden lines (black) are drawn. Spherulites crossed by the forbidden lines are not counted. The number of spherulites in each section are: A – 7, B – 11, C – 17 and D – 12, the mean number being 11.75 per section. The overall figure area, evaluated from the scale drawn the authors is $1142 \times 776 \mu\text{m}^2$. The surface density of nuclei is 5.3×10^7 nuclei/ m^2 corresponding to a volume density of $\bar{N}_t = 2.19 \times 10^{11}$ nuclei/ m^3 .

References

- (S1) Muthukumar, M. *Nucleation in polymer crystallization*. Advances in Chemical Physics, **2004**, 128, 1-63.
- (S2) Malheiro, M. J. A., Martins, J. A., Cruz Pinto, J. J. C. *Thermochim. Acta* **2004**, 420, 155-161.